

The Efficiency of PV-Wireless Charging System for Electric Vehicles on Highway Roads

Habib Kraiem^{1†}, Asma Boukhchana², Ahmed Saad Eddine Souissi⁷,

Mohamed Naoui², Aymen Flah^{2,3,4,5,6}, AlWalid Amjad Almadani⁷

¹Department of Electrical Engineering, College of Engineering, Northern Border University, Arar, Saudi Arabia,

²Processes, Energy, Environment, and Electrical Systems (Code: LR18ES34), National Engineering School of Gabès, University of Gabès, Gabès, Tunisia

³MEU Research Unit, Middle East University, Amman, Jordan

⁴College of Engineering, University of Business and Technology (UBT), Jeddah, 21448, Saudi Arabia

⁵The Private Higher School of Applied Sciences and Technologies of Gabes, University of Gabes, Gabès, Tunisia

⁶Applied Science Research Center, Applied Science Private University, Amman, 11931, Jordan

⁷Department of Industrial Engineering, College of Engineering, Northern Border University, Arar, Saudi Arabia,

(alhabeeb.kareem@nbu.edu.sa, asma.boukhchana@gmail.com, Ahmed.Souissi@nbu.edu.sa, mohamednaoui60@gmail.com, flahaymening@yahoo.fr, Amjad.madani@yahoo.fr.)

†Corresponding Author; Habib Kraiem, College of Engineering, Northern Border University, 91431, Arar, Saudi Arabia,

alhabeeb.kareem@nbu.edu.sa

Received: 06.10.2023 Accepted: 16.11.2023

Abstract- Future transportation could be completely changed by combining electric vehicles (EVs) with dynamic wireless charging systems, allowing continuous driving and faster battery charging. Dynamic wireless power transfer can solve the autonomy issues with electric cars. There are some significant disadvantages to this charging gadget drawing electricity from the electrical grid. Therefore, alternative sources like PV, Wind generators are considered a possible solution. This study aims to demonstrate the potential benefits of using wireless recharge systems for electric vehicles in conjunction with renewable energy sources in this setting. In order to define the wireless recharge concept based on an alternative energy source, this document has been constructed and the necessary portions have been regrouped. The Matlab Simulink platform developed the measured data, which tests and exanimates multiple situations. This is done by evaluating how the car's speed affects the effectiveness of wireless charging and by evaluating the potential consequences of changing environmental factors like sun radiation.

Keywords Electric Vehicles, Wireless Dynamic Charging, Mutual Inductance; Highways, State of Charge.

Nomenclature List

E_0 :	Battery constant voltage,	N	Number of turns,
K_b	The polarization resistance	l	Length of the solenoid,
i^*	The filtered battery current	I_p	Primary current,
it	The extracted capacity,	S	Surface,
A	The voltage corresponding to the end of the exponential zone	μ_0	The magnetic constant.
B	The capacitance corresponding to the exponential zone	ICE	Internal combustion engine
η_b	Battery performance,	EV	Electric vehicle
t	Discharge time	V2G	Vehicle to grid
I_b :	Battery current.	G2V	Grid to vehicle
SOC	state of charge	SAE	Society of Automatic engineering
Q_{max}	The maximum capacity.	L_p, L_s	Primary and secondary Inductances
I_{sd}	The reverse saturation current,	V_{in}	Input Voltage
q	The electron charge ($1.6 \times 10^{-19}C$),	V_o	Output Voltage
K	The Boltzmann constant ($1.38 \times 10^{-23}J/K$),	M	Mutual inductance
T	The cell temperature measured in Kelvin (K),	Gv	Voltage Gain
n	The ideal factor.	Zin	Primary impedance
B	The magnetic field,	Zsec	Secondary impedance
		R_{eq}	Equivalent resistance

1. Introduction

Due to pressure on fossil fuels worldwide, many countries are turning to ecologically clean, economical, efficient, and dependable energy sources. As one of the largest sources of CO2 emissions, fossil fuels seriously threaten the environment. The percentage contribution of CO2 emissions by the electricity and heat sector is major in the transportation, industrial, housing, and other regions, claims the International Energy Agency[1], [2], [3]. The transportation sector seems to be alleviated as many other solutions come in the recent research, which can give a solution for gaz emission reduction. Electric vehicles (EV) are currently growing rapidly as a result of five important trends around the world: the depletion of fossil fuels and the associated rise in fuel prices; the public's growing knowledge of and desire to tackle climate change; the development of new commercial effectiveness of technology for renewable energy; he advancement of electric motors and electronic control systems that directly manage EV propulsion; and improvements in EV enabling technologies like Vehicle-to-Grid (V2G) and Grid-to-Vehicle (G2V) [4],[5], [6].

Much work has been done to integrate environmentally friendly energy sources like solar and wind power. The transition from petrol-fueled mobility to electric mobility is the current trend in transportation. The two tendencies could be combined to create an electric mobility system that uses green energy and 0% of gaz emission can be touched [7].

The two main disadvantages of electric vehicles over conventional vehicles are their short driving range and high price resulting from current battery technology and specifications. Increasing driving range and/or reducing battery size is possible with the widespread use of on-road charging facilities. Therefore, such systems offer a solution to overcome the existing electric mobility limitations.

Charging systems are the primary factor influencing the growth of EV. Static charging is frequently regarded as a viable temporary measure to counter low-voltage grid congestion from EV charging, thereby circumventing hefty grid upgrade expenses. Studies [8] and [9], the efficacy of static charging schedules for EVs is highlighted as a short-term remedy for grid congestion. These researches juxtapose static and dynamic charging techniques, delving into the advantages and drawbacks of each. On the other hand, as elaborated in [8], dynamic charging enables EVs to recharge in moving, fostering power interaction between the vehicle and the grid without the need for stationary charging infrastructures. This method boasts numerous benefits, such as enhanced energy transfer efficiency, negligible vehicle downtime during charging, and a diminished environmental footprint as noted in [10]. Given these advantages, our research predominantly leans towards the dynamic charging strategy.

In this work we are interested in wireless dynamic charging technology, this technology offers faster driving without having to stop to recharge in conjunction with electric vehicles and automated and connected vehicles [11], [12]. Inductive coupling is one of the most often used techniques for dynamic wireless charging systems to supply energy from

the transmitting coils located on the road to the receiving coils located under electrical vehicles. According to Figure 1, the transmitters and receivers build a loosely coupled transformer that delivers power by mutual inductance across an air gap.

This study used photovoltaic panels to power the wireless dynamic charging system. These generate the DC current. They are connected by a converter boost to increase the supply voltage from that of the load. This converter is connected to the inverter, which converts the DC into AC current to power the coil issuer [13], [14], [15] . This creates a magnetic field, which converts magnetic energy into energy to power the take-up reel. This coil is linked to the rectifier which converts AC current into DC current to charge the electric vehicle's battery.

The authors of studies [16], [17] and [18] delved into different coil designs for wireless power transfer in electric vehicle battery charging. A comparative analysis of various coil shapes was presented in [18] . Utilizing Ansys for modeling, they assessed the performance of both circular and rectangular coils. The findings underscored the superiority of the rectangular coil over the circular design and other shapes. As a result, our research predominantly concentrates on the design of rectangular coils.

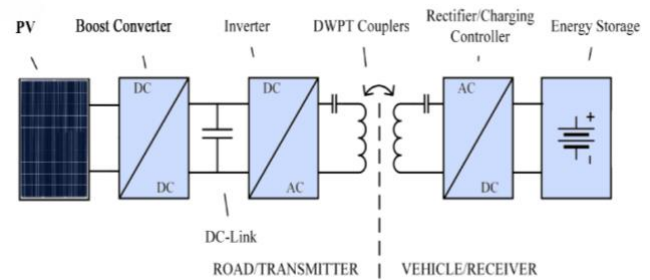


Fig. 1. An electric vehicle wireless charger's structural design.

Infrastructures for public and private charging must be established with sufficient coverage to provide the push needed for the arrival of EVs.. These recharging infrastructures may be supplied by the electrical grid or by renewable energy sources. The modalities of recharge (fast or gradual) may differ during the use of these various energy sources, necessitating the sizing of recharge systems and the modification of installations. The propulsion systems for electric vehicles often include a few components that work together to maintain the vehicle's high power and road stability. The charging mechanism is coupled to most of these components. In this approach, the power transfer without a dynamic link is useful for handling electrical vehicle issues. However, there is a major disadvantage to this recharge system's link to the energy source of the electrical network. In studies [19], the authors utilized the electric grid to power electric vehicle charging systems. Often, these grids rely on fossil fuels for electricity generation, which negatively impacts the environment[20], [21]. To address this concern, our approach shifts away from grid energy, emphasizing the use of solar energy for EV charging, [22], [23]. Wireless charging has long been common with fully electric automobiles. That is designed to enable battery recharging

while the car is in motion. This method's complex working philosophy, which involves the existence of several variables and parameters, makes it difficult to examine. In addition, a variety of other criteria, like the vehicle's speed and the widths and lengths of its receptacles, depend on the condition of the vehicle—whether it is moving or not. It offers a novel approach to improving the effectiveness of dynamic wireless charging technology [24].

This work aims to characterize the different factors that may respond to the wireless recharge system's performance. The paper's goal is further developed in light of the study's findings.. This was studied by testing different architectures and concepts that can be used for charging the vehicle in wireless mode. Even though previous results have demonstrated that the wireless recharge technology can be profitable, some weaknesses have appeared if the highway roads are in question for making this technology for users. The major problem is the requirement for electrical power to supply the recharge system. On highway roads, this is not always available. For this reason, PV systems have been highlighted in this study as a sustainable and alternate energy source. This research aims to investigate this intricate structure. Therefore, the built paper regroups seven sections. After the primary introduction, the EV wireless model is discussed and then, in the third part, the renewable energy source, adapted for the application is discussed. In section four, the built wireless recharge model is presented and exposed. In section five, the simulation results, which describe the overall process are summarized and discussed. Next, the conclusion and the perspectives of the exposed work are shown.

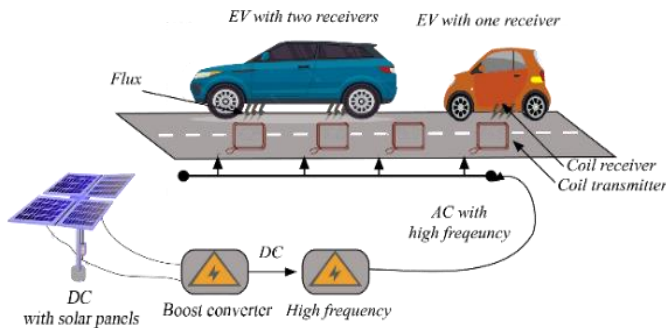


Fig. 2. The wireless charging system's composition: from PV to load

2. EVs wireless charger operation

2.1. The Wireless Recharge Concept

The two primary components of wireless power transfer technology that are the subject of this study are one for the highway and one for the vehicle. The part of the road that is permanently fixed is the transmitter. The second part, which is situated below the car, is the moving receiver. Each component has its own electronic system, and a vacuum separates the two components. The transmitter block generates a high-frequency, alternating magnetic flux. This magnetic flux, which the receiver coil connects to and then transforms into electric energy, is utilized to refuel the electric vehicle's battery. Two electric vehicle (EV) examples with

wireless charging stations are shown in Figure 2. They are both parked on a road.

The functional layout of the electric vehicle's wireless charger is shown in Figure 3. The input DC voltage source, or V_{in} , is defined by the Society of Automotive Engineers (SAE) J2954 standard as having a typical range of 350 to 500 VDC. The primary inductance (L_p) displays the self-inductance of the transmitter coil, the secondary inductance (L_s) displays the self-inductance of the receiver coil, and M represents the mutual inductance between the transmitter and the receiver. A boost converter normally generates the input voltage V_{in} , and an inverter is used to transform the input voltage (V_{in}) into an alternative high-frequency voltage fed to the primary compensation tank, consisting of capacitive and inductive resonances. The primary resonant tank serves as a limited filter, allowing fundamental-frequency signals to pass while blocking elevated frequencies, and compensates for the reactive power of the magnetic coupler's significant coupled inductor. Therefore, voltage AC is used to power the primary coil. The wireless charging system's output power is inversely proportional to the transmitter current [25]. The transmitter current is commonly kept constant to simplify the output power control technique. The secondary side of the system receives a second resonant tank to increase system efficiency and power transmission capacity. Also, it eliminates the magnetic coupler unit's substantial leakage inductance. After passing through the resonant tank, an inverter solves the induced voltage at the reception coil. In contrast to the conductive charger, the primary side of the wireless charger is positioned on the vehicle while the secondary side is located off-board [26], [27].

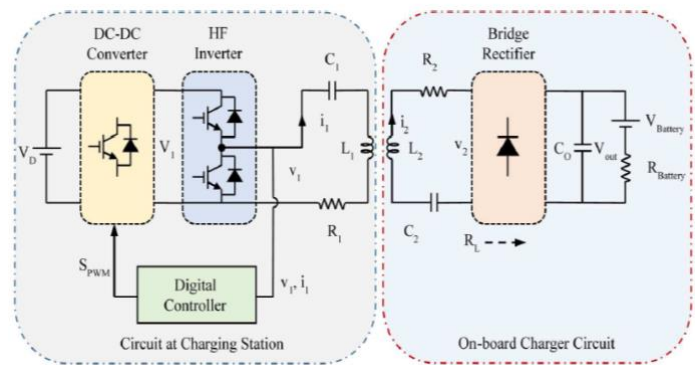


Fig. 3. Diagram block of the onboard EV wireless charger.

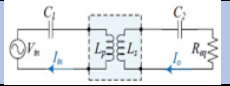
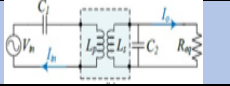
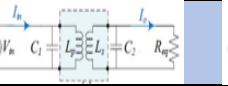
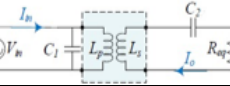
2.2. Topologies for Compensation

The wide gap causes the primary and secondary sides' connection to be weak. Because of the high reactive power, it is necessary to use resonance elements on both sides as compensation to retain optimal efficiency and achieve the desired level of transferred power. It is also necessary to modify the output parameters on the load side to guarantee that the charger functions at a particular voltage with the current the battery needs. The inductive energy transfer system might be used with either of the four resonant circuit topologies. They are called parallel (P) or series (S) connections

depending on where the capacitor resonance is inserted on each side. The Table 1 shows the representation of different strategies of compensation: SS, SP, PS and PP [28],[29]. Inductances (L_p, L_s) and (C_1, C_2) are selected to cancel the reactive portion of the transferred power. Reduce the apparent power from the source of entry and ensure that the active power is transmitted to the load to improve power transfer [30], [31], [32]. Each circuit's voltage gain (G_v) is defined as the proportion of the input voltage (V_{in}) to the output voltage (V_o). It is crucial to recognize the crucial variables of input impedance, efficiency, and output voltage gain ($G_v = \frac{V_o}{V_{in}}$)

) to analyse any resonant architecture. The input impedance can be used to calculate the input phase angle, input current, and voltage gain as a function of the resonant elements. It is anticipated that efficiency and voltage gain will depend less on the coupling factor with a misalignment-tolerant design. Table 2 summarizes the most popular topologies' input impedances, output voltage gains, and schematics.

Table 1. Wireless charging features.

Design				
Topologies	SS	SP	PP	PS
Power transfer ability	****	****	**	**
Ability to use electric vehicles	****	****	***	***
Dimensional tolerance	****	****	***	***
The impedance of the resonance condition	**	**	****	****
Distance sensitivity of the power factor	**	**	***	***
Performance tolerance for frequency	**	****	**	****
Sources	[33],[34]			

Remark: **** : high, ***: medium, ** low

Table 2. Several typical resonant topologies are defined by voltage gain and impedance.

Topology	Voltage Gain (G_v)	Impedances
SS	$\frac{M\omega R_{eq}}{ Z_{in} Z_{sec} }$	$Z_{in} = \frac{1}{j\omega C_1} + j\omega L_P + Z_r$ $Z_{sec} = j\omega L_s + \frac{1}{j\omega C_2} + R_{eq}$
SP	$\frac{M\omega R_{eq}}{ 1 + j\omega C_2 R_{eq} Z_{in} Z_{sec} }$	$Z_{in} = \frac{1}{j\omega C_1} + j\omega L_P + Z_r$ $Z_{sec} = (R_{eq}^{-1} + j\omega L_s^{-1} + j\omega C_2^{-1})^{-1}$
PP	$\frac{M\omega R_{eq}}{ 1 + C_1\omega(Z_r + j\omega L_p) 1 + j\omega C_2 R_{eq} Z_{in} Z_{sec} }$	$Z_{in} = (j\omega C_1 + \frac{1}{j\omega L_P + Z_r})^{-1}$ $Z_{sec} = (R_{eq}^{-1} + j\omega L_s^{-1} + j\omega C_2^{-1})^{-1}$
PS	$\frac{M\omega R_{eq}}{ 1 + C_1\omega(Z_r + j\omega L_p) Z_{in} Z_{sec} }$	$Z_{in} = (j\omega C_1 + \frac{1}{j\omega L_P + Z_r})^{-1}$ $Z_{sec} = j\omega L_s + \frac{1}{j\omega C_2} + R_{eq}$
References	[35]–[37]	

2.3. The Concept of Wireless Charging's Mathematical Model

There are two types of charging: static charging, which several companies use and continue to develop. We use the Waseda Electric Bus in Japan as an example, which has a power range of 30 to 150 kW and 105 mm between the transmitter and receiver coils. While using this approach, the car charges every time it passes by a bus stop [36], [38].

Dynamic charging is the second kind of charging. Under this charging method, the vehicle charges while in motion. This is accomplished using a specially designed track that has coils placed throughout it that only become active when a passing vehicle passes. With this approach, it may be possible to lower the vehicle's battery capacity and, as a result, its weight and cost.

A condensed illustration of this wireless charging technology is shown in Figure 3. The input and output voltages of this technology are denoted V_p and V_s as shown in equations (5) and (7) [39].

The magnetic coupling coefficient is related to the mutual inductance by equation (1)

$$C_k = \frac{M}{\sqrt{L_p L_s}} \tag{1}$$

Z_r is used in equation (2) to represent the reflected impedance from the secondary to the primary:

$$Z_r = \frac{\omega^2 M^2}{Z_s} \tag{2}$$

By using the selected compensation topology, Z_s is the secondary impedance, and the following equation (3) provides the current flowing through the secondary winding:

$$I_s = \frac{j\omega M I_p}{Z_s} \tag{3}$$

Equation (4) indicates that the primary and secondary resonant frequencies are the same:

$$\omega = \frac{1}{\sqrt{C_{(p,s)} L_{(p,s)}}} = 2\pi f \tag{4}$$

or:

$C_{(p,s)}$: Primary and secondary capacitor.

$L_{(p,s)}$: Primary and secondary inductance.

The primary and secondary voltages can be written as follows:

$$\begin{cases} V_p = j2\pi f_r L_p I_p - j2\pi f_r M I_s \\ V_s = j2\pi f_r M I_p - j2\pi f_r L_s I_s \end{cases} \tag{5}$$

The primary and secondary power equation is in (6):

$$\begin{cases} P_p = V_p I_p \\ P_s = V_s I_s \end{cases} \tag{6}$$

The magnetic flux transmitted for the transmitting and receiving coil positions is displayed in Figure 4. Greater flux and energy transmission occur when there is less space between the centers of the two coils [39]. The percentage ratio is a factor important to consider when determining how much power the receiver has.

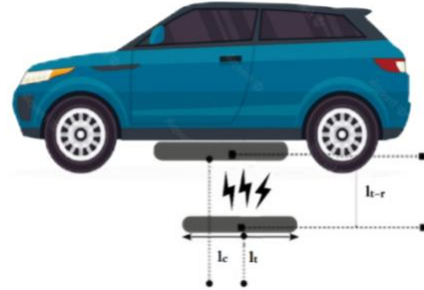


Fig. 4. The primary coil's magnetic flux transmission.

The primary coil's proportional flux is expressed in equation (7) as a function of related physical variables. This equation assumes that the centers of two coils are matched to allow proper transmission of magnetic flux. The flux ϕ_s obtained in the secondary coil "attached to the vehicle" in the mobility example, however, is described as the goal of the first flux established if the two coils are jumbled.

$$\begin{cases} \phi_p(t) = \left(\frac{\mu_0 \cdot S \cdot N^2}{l}\right) I_p(t) \\ \phi_s(t) = \epsilon \cdot \phi_p(t) \end{cases} \tag{7}$$

The new dynamic model method of the wireless charging system is based on the parameter ϵ . The following table 3, presents the relation between the parameter ϵ , the length l_{t-r} between the transmitter coil and the receiver coil, the length l_c that defines the offset between the centers of two coils and the length of the transmitter coil l_t .

Table 3. The relationship between the parameter ϵ and the lengths that define the magnetic field.

Parameter ϵ	dimensions l_{t-r} , l_c and l_t
$\epsilon = 0$	$l_c > l_t$
$\epsilon = 1$	$l_c = 0$
$0 < \epsilon < 1$	$0 < l_c < l_t$

The inductance factor "L" is related to the shape of the coil; in this case, the shape is flat rectangular. Therefore, so, "L" can be expressed as follows:

$$L = K_1 B_0 \frac{N d_m}{1 + K_2 \rho} \tag{8}$$

K_1 and K_2 denote the empirical coefficients ($K_1=2,34$ and $K_2=2,75$), B_0 presents Vacuum permeability ($B_0 = 4\pi \cdot 10^{-7} \text{H/m}$), d_m is the average diameter, and ρ presents in (9), exposes the rate at which the coil is being filled.

$$\rho = \frac{d_{out} - d_{in}}{d_{out} + d_{in}} \tag{9}$$

The filling rate ρ reflects how hollow the spiral is. In the case of a small model ρ , the coil is hollow ($d_{out} \approx d_{in}$) and in the case of a large model ρ , the coil is full

$(d_{out})d_{in}$). The following figure 5 shows the winding characteristics.

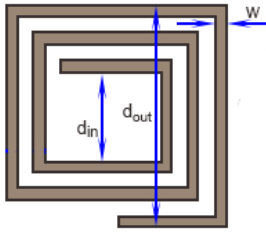
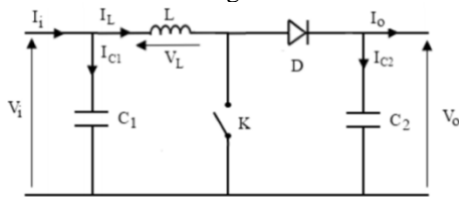


Fig. 5. Winding characteristics.

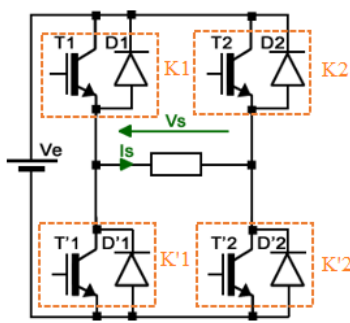
2.4. The associated converters

As mentioned in the paper's purpose, the main goal of this study is to offer a method for providing the required power to a wireless transmitter that is located on a long road. The appropriate DC/DC converter will be installed first to make the relationship with the PV panels. Then, the DC/AC inverter will be installed to manage the first transmitter's needed frequency signal. The relevant converter designs and interactions are shown in Figure (6) [27], [40], [41].

- The boost converter is typically used to convert a low input voltage to a high output voltage. It has an input voltage V_i source DC, an inductance L , a switch K , a diode D , and two capacitors C_1 and C_2 . Figure 6.a designs the equivalent electrical diagram of the boost converter.



(a) Converter DC/DC.



(b) Inverter design

Fig. 6. Appropriate Converters.

The corresponding duty cycle is expressed as follows:

$$\frac{V_o}{V_i} = \frac{1}{1-D} \tag{10}$$

Equations 11 and 12 give the expression for capacitance and inductance respectively of the needed filter [42]:

$$C = \frac{DV_o}{f_s R \Delta V} \tag{11}$$

$$L = \frac{DV_i}{f_s \Delta I} \tag{12}$$

The corresponding equation depends on the switch K position, So:

If the switch K is open or closed, the equations can be expressed as in (13) and (14) respectively:

$$\text{If } K \text{ is On then } \begin{cases} I_{c1} = C_1 \frac{dV_i}{dt} = I_i - I_L \\ I_{c2} = C_2 \frac{dV_o}{dt} = I_L - I_o \\ V_L = L \frac{dI_L}{dt} = V_i - V_o \end{cases} \tag{13}$$

$$\text{If } K \text{ is OFF then } \begin{cases} I_{c1} = C_1 \frac{dV_i}{dt} = I_i - I_L \\ I_{c2} = C_2 \frac{dV_o}{dt} = -I_o \\ V_L = L \frac{dI_L}{dt} = V_i \end{cases} \tag{14}$$

- The second converter part is the inverter that provides a single-phase alternating voltage at its output. To assemble the power circuit of the inverter. Figure 6.b shows the inverter wiring diagram (DC/AC converter).

The states of the switches can be determined by the value at the terminals of the load type as an inductive case:

If K_1 and K'_2 are ON while K_2 and K'_1 are off, therefore the outputted voltage is expressed as follows:

$$V_s = L \frac{di}{dt} + Ri = V_e \tag{15}$$

For the other combination, the outputted voltage and current will be as follow;

$$V_s = L \frac{di}{dt} + Ri = -V_e \tag{16}$$

Finally, the expression of the current is in (17)

$$i(t) = \frac{V_e}{R} \left(1 - e^{-\left(\frac{t-T}{\tau}\right)} \right) + I_M e^{-\left(\frac{t-T}{\tau}\right)} \tag{17}$$

2.5. The Power Storage System

The main battery design is exposed as it is formulated in equation (18). A DC voltage source and a variable resistor placed in series form the model, where the charge/discharge voltage of the lithium-ion battery is described [32].

$$V_t = \begin{cases} V_{b\text{-charge}} = V_{oc} + R_0 I_L \\ V_{b\text{-décharge}} = V_{oc} - R_0 I_L \end{cases} \tag{18}$$

The state of charge SOC can be expressed as:

$$SOC\% = \left(\frac{Q(0) \int_0^t (n_b I_b) dt}{Q_{max}} \right) \cdot 100 \tag{19}$$

The battery voltage charge and discharge (V_{oc}) is specified by the internal elements of the battery and is expressed as:

$$V_{oc} = \begin{cases} E_0 - K_b \left(\frac{Q}{Q-it} \right) i^* - K_b \left(\frac{Q}{Q-it} \right) it \\ + Ae^{(-B.it)} \rightarrow \text{discharge } i^* > 0 \\ E_0 - K_b \left(\frac{Q}{0.1Q+it} \right) i^* - K_b \left(\frac{Q}{Q-it} \right) it \\ + Ae^{(-B.it)} \rightarrow \text{charge } i^* < 0 \end{cases} \quad (20)$$

3. Source of Power Description

3.1 Concept of PV for Feeding the Wireless Recharge: Discription

Suppose this autonomous recharging topology is used over 100 km of road. In that case, a significant number of PVs will be required, making this a potentially significant PV project that will require substantial funding to be completed. From the other point of view, it is important to mention that it is possible to use the PV generator system to cover the breakdown of the grid, which can help improve global electricity production. Because PV-wireless charging infrastructure makes it easier for customers to use EVs on highways, it will improve global EV sales.

It is known that generating power from renewable energy such as PV or wind greatly impacts the global environment by reducing gas emissions when electricity is produced. This solution has an indirect impact on global gas emissions. If this topology is dominated, the EV number will be higher, as more recharge solutions for EV recharge exist even if the car is in movement, reducing the traditional vehicle number. This impacts gas emission, especially if we know that more than 30% of gas emission comes from vehicles.

The most important factors, that can influence the efficiency of the proposed EV charger solution are related to the external climatic conditions, such as the temperature or the dust. It is known that even if the temperature is high, or even if the PV panel is not cleaned the PV power production decreases and this will decrease the level of power given to the wireless coils. Vehicle speed is also a factor that can make the wireless recharge solution not interesting on highway roads. It is described in this study that even if the vehicle speed is high, then more coils need to be used as transmitters. This will complicate the wireless recharge solution and make the system obfuscate. According to the study's findings, the worldwide efficiency of the suggested EV recharge method can be influenced by both the vehicle's speed and the weather.

3.2 Mathematical Modeling

As it has been exposed before, Solar energy will be managed to be the main energy source for this recharge system. So, firstly a description of the PV solar will be done. Then, we try to describe an overall PV panel model. A PV module is formed of several PV cells connected in series and parallel to produce the necessary voltage and current levels.

The general model's equivalent circuit is composed of a photocurrent (I_{ph}), a diode current, a parallel resistance (R_{sh}) that expresses a leakage current, and a series resistance (R_s) brought on by the contacts between semiconductors and metallic parts [43],[44].

The following equation will get the current:

$$I_c = I_{ph} - I_D - I_{sh} \quad (21)$$

Where I_{ph} is the photocurrent produced by light and I_{sh} is the parallel resistor current, which can be calculated as:

$$I_{sh} = \frac{V_c + R_s I_c}{R_{sh}} \quad (22)$$

The saturation current is proportional to the diode current I_D . The following equation gives the value of this magnitude:

$$I_D = I_{sd} \times \left[e^{\left(\frac{q(V_c + R_s I_c)}{n \cdot k \cdot T} \right)} - 1 \right] \quad (23)$$

According to the equation below, solar radiation and cell operating temperature have a major role in determining the photocurrent:

$$I_{ph} = [I_{sc} + K_i(T - T_{ref})] \frac{G}{G_{ref}} \quad (24)$$

Taking into account the same brightness and temperature over the entire panel, the generated current can be described as follows [45]. N_s is the serial number of the PV panels and N_p is the parallel number .

$$I_{PV} = N_p \left(I_{ph} - I_{sd} \cdot \left[e^{\left(\frac{q(V_c + R_s I_c)}{n \cdot k \cdot T} \right)} - 1 \right] \right) - \left(\frac{N_p V_c + R_s I_c}{R_{sh}} \right) \quad (25)$$

4. Wireless Charging System: Proposed Concept

ANSYS Maxwell was used to create the 3D model of the transmitter and receiving coils. The two copper coils are 20 centimetres apart. To record the magnetic field created between the two coils, a clear rectangular plate was placed between them. The related plat specifications are summarized in table (4).

Table 4. Rectangular plate components and coil specifications.

Name	Value
Position (cm)	-30,-30,10
X Size (cm)	60
Y Size (cm)	60
W_p	2,5 cm
Air gap:g	20 cm
Reference	[46]

The simulations would be run in a space that measures (120 cm, 240 cm, and 120 cm). Setting a boundary for the two coils' locations is the solution created by the ANSYS Maxwell software. Figure 7 illustrates the transmitter and receiver coil designs. Tables 4 and figure 8, provide a summary of the corresponding parameters for the coils.

In ANSYS Maxwell, figure 8 shows the transmitter and receiver coils, as well as their magnetic fields. The magnetic field between the coils decreases when the distance between them is larger. We have discovered that the coupling coefficient between the two coils increases as the distance between them decreases. The amount of mutual inductance between the coils changes slightly, as shown in figure 9, because each coil corresponds to the sum of its own inductance and the mutual inductance of the other coil. The definition of the excitation current track causes a small change in rate when the other coil approaches since there is still some flux.

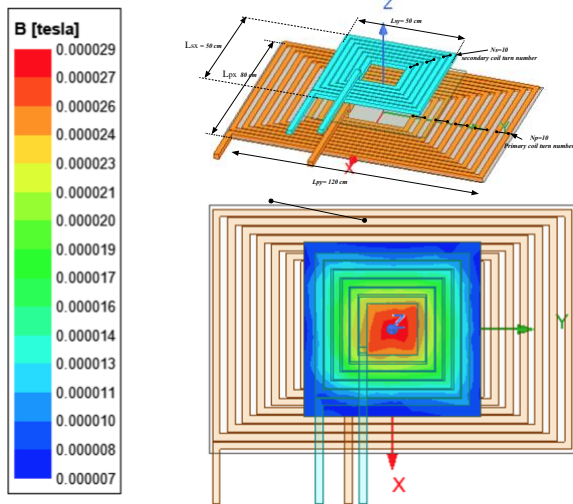


Fig.7. The magnetic field between the transmitter and receiver coils and the 3D model specifications

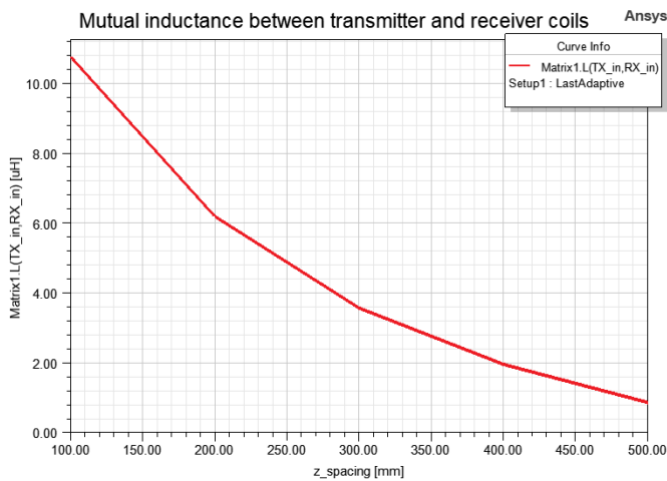


Fig. 8. Mutual inductance between transmitter and receiver coils.

To create the overall schematic for the wireless charging system, ANSYS Electronics software was used. Figure 9 shows the wireless charging setup with SS topology. In the primary part, on an energy source of frequency 150kHz and voltage 280V. Based on the simulation results, the input/output voltage amplitude marge is 279.96/ 257.23 V and the corresponding (input current is 85.36A and the output current is 85.74A).

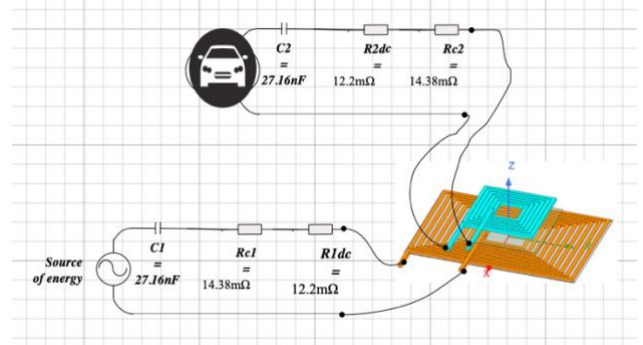


Fig. 9. Wireless charging system with the SS compensation method.

So, the corresponding input and output powers are both present as steady-state waves in figure 10. There is a maximum input power of 53.7 KW and a maximum output power that is greater than that. The results of the calculated ratio of input to output powers indicate that the performance is roughly 87.82 percent.

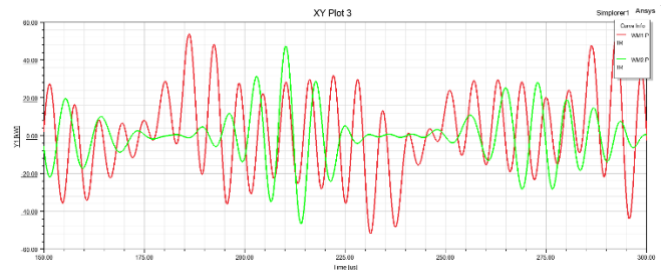


Fig. 10. The input and output power curves.

As it is in figure 11, The studied highway was supposed to compose a double line. One of them is provided by the wireless recharge system. Each specific number of this transmitter has been supposed to be connected to a PV panels system. As static specifications, for each 10 kilometer stretch of highway, 5000 transmitter coils of 120 cm in length are used, with a distance of 80 cm between them, as shown in Figure 11. The infrastructure for wireless charging that is installed on public roads will ultimately decide the charge density and power transfer charges. Two potential conceptualizations of the system exist [35].The maximum power transfer rate is 100 KW. Assume that there is sufficient electricity in the first scenario to power two electric automobiles across a distance of 50 meters. In Layout 2, there is an electric vehicle every 40 meters, with a 140 KW maximum power transfer rate.

Since there is a solar central plant for every kilometer of a highway in this study, the power will be controlled to the transmitter by means of an ensemble of switchers on each coil to facilitate the convenient switching between them while the vehicles are being charged. The prototype is depicted in Figure 13. This version does not address the intelligent power management algorithm. If a power management tool controls the various inverters and determines which inverter should be connected based on whether a vehicle needs to be charged or not.

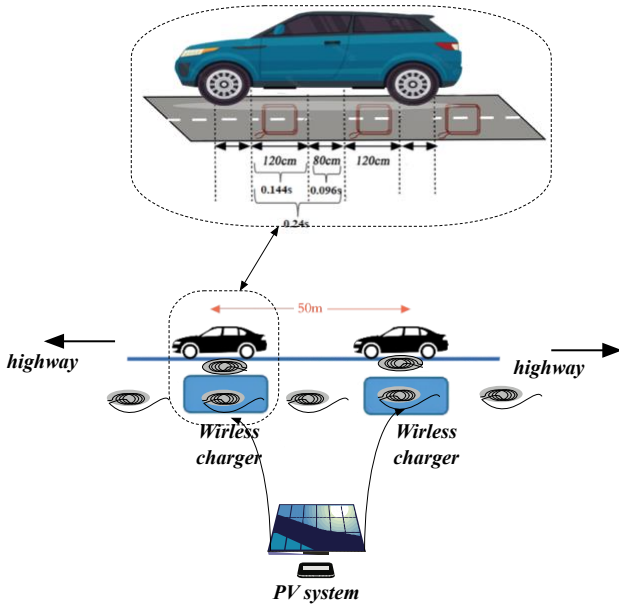


Fig. 11. Arrangement in the highway and coils placements around the vehicle and on the highway.

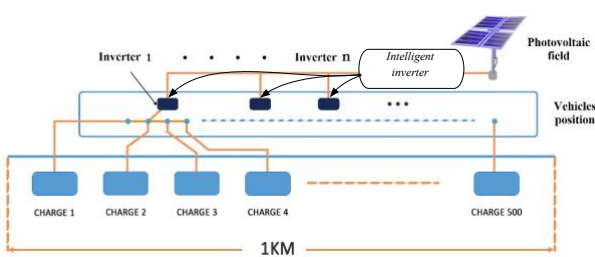


Fig. 12. Global architecture for transmitters and PV panels.

5. Results discussion

5.1 Simulation Conditions

We assessed the overall performance and efficiency of the system with the Matlab simulation software, which is installed in an I7 processor with 16 GO as a Ram memory. The outcomes have really been shown for the scenario of an electric car with a wireless charger that travels one kilometer on a highway. 500 coil transmitters are found every one kilometer. In the simulation steps, the vehicle speed was varied from 30 to 100 km/h, and based on the build mathematical model, the needed coil transmitter number was evaluated for reaching a full battery charge. In the second step, the PV-wireless recharge system was evaluated by making a variation on the irradiation factor from 60%, 80% and 100%. The simulation conditions were based on an initial battery state of charge equal to 50%, a vehicle weight equal to 750Kg, no road slope existing and a constant drive cycle was applied. The coils' dimensions, size and position on the road are summarized in Figure (7). After positioning all of this information on the Matlab code, the esteemed coil number, the needed recharge time and more other statistics can be depicted for a various vehicle speeds. Figure 13, gives these details. The results analysis was built to show the various statistics for having a full recharge vehicle and the importance of the case where two possible transmitter/ receiver coils are used for the same vehicle.

5.2 Simulation Discussion

The findings demonstrate that the 120 cm transmitter coil can recharge the car in 0.144 seconds at a 30 km/h speed, as illustrated in Figure 13. Therefore, the recharge period for a 1 kilometer length with 500 coils is 120s. This figure demonstrates that the time required to recharge the battery decreases with increasing vehicle speed. Based on the fastest recorded speeds, which come in at 30 km/h. The car would pass through the recharge zone in one minute and twenty minutes. In other words, the car will spend 0.24 seconds wirelessly connected to each transmitter.

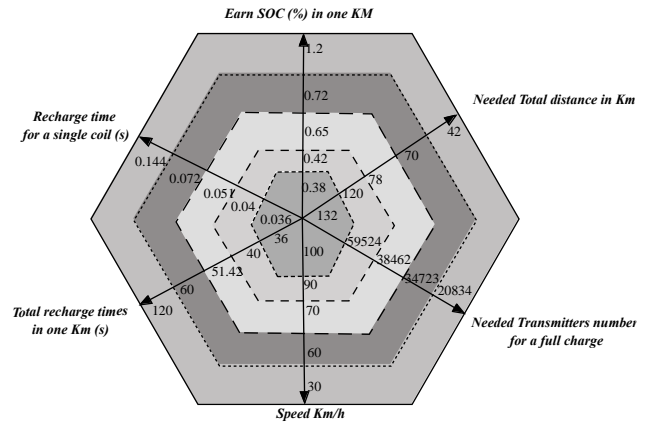


Fig. 13. For an EV to be fully charged, the required number of kilometers for a wireless recharge road is 50% of the starting state of charge and a full radiation factor.

According to the simulation rules, the distance between the transmitting and receiving coils affects how much power is delivered. Figure (14), gives the related mutual inductance concerning the case of if only one transmitter is used or two transmitters are used for feeding the vehicle by the power. It is clear that if two coil receivers/transmitters are used, better performances will appear. The maximum connection can be seen at 70 mm and -110 mm, equivalent to the two coil centers. The point Zero was selected as the center, which is in the middle position between the two coils.

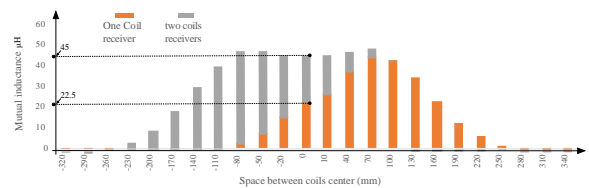


Fig. 14. mutual inductance in the case of one or two transmitter/receiver coils used for charging the vehicle.

As previously revealed, it appears that a single car with two coils serving as both a transmitter and a receiver can achieve better results. For this reason, figure (15) shows a better State of charge evolution in the case of two coils. The statistics following the simulation phase are shown in Figure (13). For the best efficiency factor irradiation, based on these specifications and focusing on the lowest studied speed (30 km/h), the battery state of charge will change by up to 0.05 percent in 5 seconds for the case of one coil and by 0.1 percent

for the case of two coils. With one coil, the battery can reach a new state of charge (SOC) of 51.2 percent, and with two coils, it can reach 52.4 percent, provided that the driving

technique, vehicle speed, and solar radiation factor remain constant.

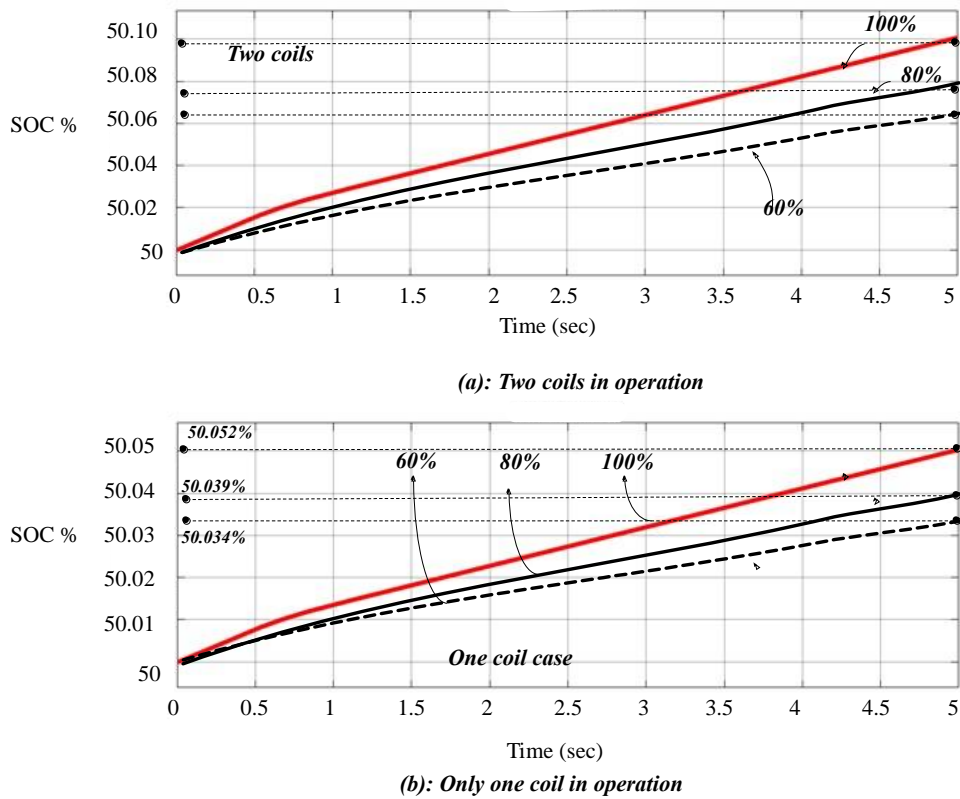


Fig. 15. SOC evolution for three irradiation factors and a simulation time of five seconds under 30 km/h. when there is only one transmitter / receiver (b) or two transmitter/receiver coils (a) in operation.

Viewed from the opposing angle, the rentability of the system may be impacted by solar radiation. The required complete recharge time will automatically increase in cases where the Earned SOC can drop by at least 0.02 percent as the case of a radiation factor is equal to 60%.

5.3 Results Summarizes

The results demonstrate that should the wireless recharge tool be chosen, the integration of the PV system for vehicle charging must meet several specifications and best performance requirements to function well.

The outcomes can be listed as four points as follows:

- Both the number and size of coils have an impact. The results from figure (15) demonstrate that the required recharge time will reduce when two coils are employed compared to when only one receiver coil is used.
- The status of charge is significantly impacted by the PV radiation factor, and higher radiation factors are correlated with better conditions.
- It was discovered that vehicle speed also had a significant impact on the overall recharge tool performances, with the lowest selected speed showing the best results.
- Furthermore, we've come to the conclusion that the total number of transmitter coils needs to be chosen for the fastest vehicle speed feasible, which could complicate the entire road trajectory.

For the cited simulation conditions, The study aims to outfit 157 kilometers with over 78,000 transmitters so that, if the battery SOC starts at 50%, the entire battery can be recharged.

6. Perspectives of the Exposed Work

This study investigates the potential benefits of lowering reliance on the electrical grid and guaranteeing the continuous charging of electric vehicles by utilizing renewable energy sources, such as PV generators, in wireless charging systems. Furthermore, this study can assist in increasing the effectiveness of the wireless charging system and solve safety issues by evaluating how various factors, such as vehicle speed and environment, affect its performance. All things considered, the study offers a foundation for creating and implementing PV-wireless charging systems for electric cars on roads that are more efficient and ecological. Conversely, a crucial query to consider is how the research addresses the safety concerns brought up by the use of PV-wireless charging systems on public roads. To address this and allay safety concerns, photovoltaic (PV) generators can be used as a substitute power source for wireless charging systems. By utilizing renewable energy sources, producing electricity from solar energy lowers carbon emissions and advances sustainability.

7. Conclusions

In-depth research on dynamic wireless power transmission for a highway application is designed and studied in this work. The system's current state and its relevance to EV applications were described. Every component of this recharge system has its mathematical block explained and examined in order to properly complete the system examination. The efficiency of the recharging system was thoroughly tested using ANSYS Maxwell and Matlab Simulink, two simulation tools, at different speeds and with a renewable energy source based on solar radiation.

Additionally, this study has shown that a variety of elements can react to the global system, making it difficult to estimate the required number of transmitters in the event that the vehicle-driven mode deviates from accepted norms or the climate factor changes.

Acknowledgements

The authors gratefully acknowledge the approval and the support of this research study by the grant no ENGA-2022-11-1483 from the Deanship Of Scientific Research At Northern Border University, Arar, K, S, A

8. REFERENCES

- [1] A. AlKassem, M. Al Ahmadi, and A. Draou, "Modeling and Simulation Analysis of a Hybrid PV-Wind Renewable Energy Sources for a Micro-Grid Application," in *2021 9th International Conference on Smart Grid (icSmartGrid)*, 2021, pp. 103–106.
- [2] M. Akil, "A coordinated EV Charging Scheduling Containing PV System," *Int. J. Smart grid*, vol. 6, no. V6i3, 2023.
- [3] S. M. Arif, T. T. Lie, B. C. Seet, S. Ayyadi, and K. Jensen, "Review of electric vehicle technologies, charging methods, standards and optimization techniques," *Electronics*, vol. 10, no. 16, p. 1910, 2021.
- [4] H. Oufettoul, S. Motahhir, I. A. Abdelmoula, G. Aniba, W. Issa and O. Mahir, "Optimum MPPT Technique for Reconfiguring the Photovoltaic Array Under Partial Shading Failure," *2023 12th International Conference on Renewable Energy Research and Applications (ICRERA), Oshawa, ON, Canada, 2023*, pp. 331-338.
- [5] A. Mahesh, B. Chokkalingam, and L. Mihet-Popa, "Inductive wireless power transfer charging for electric vehicles--a review," *IEEE Access*, vol. 9, pp. 137667–137713, 2021.
- [6] E. Giannakis, D. Serghides, S. Dimitriou, and G. Zittis, "Land transport CO2 emissions and climate change: evidence from Cyprus," *Int. J. Sustain. Energy*, vol. 39, no. 7, pp. 634–647, 2020.
- [7] T.-E. Stamati and P. Bauer, "Green energy for on-road charging of electric vehicles," in *Proceedings of 15th international conference MECHATRONIKA*, 2012, pp. 1–9.
- [8] L. A., J. Jiang, A. Maglaras, F. V., and S. Moschoyiannis, "Dynamic wireless charging of electric vehicles on the move with Mobile Energy Disseminators," *Int. J. Adv. Comput. Sci. Appl.*, vol. 6, no. 6, 2015.
- [9] P. Hogeveen, M. Steinbuch, G. P. J. Verbong, and A. Wargers, "Revisiting static charge schedules for electric vehicles as temporary solution to low-voltage grid congestion with recent charging and grid data," *Sustain. Energy, Grids Networks*, vol. 31, 2022.
- [10] A. A. S. Mohamed, A. A. Shaier, H. Metwally, and S. I. Selem, "An Overview of Dynamic Inductive Charging for Electric Vehicles," *Energies*, vol. 15, no. 15, 2022.
- [11] M. Akil, E. Dokur and R. Bayindir, "Impact of Electric Vehicle Charging Profiles in Data-Driven Framework on Distribution Network," *2021 9th International Conference on Smart Grid (icSmartGrid)*, Setubal, Portugal, 2021, pp. 220-225,
- [12] N. Priyadarshi, P. K. Maroti, and M. G. Hussien, "Extensive performance investigation of Luo converter-based modified firefly maximum point tracking algorithm for permanent magnet synchronous motor-driven photovoltaic pumping system," *IET Renew. Power Gener.*, vol. n/a, no. n/a, Jun. 2022.
- [13] N. Priyadarshi, P. Sanjeevikumar, M. S. Bhaskar, F. Azam, I. B. M. Taha, and M. G. Hussien, "An adaptive TS-fuzzy model based RBF neural network learning for grid integrated photovoltaic applications," *IET Renew. Power Gener.*, vol. 16, no. 14, pp. 3149–3160, Oct. 2022.
- [14] R. Reshma Gopi and S. Sreejith, "Converter topologies in photovoltaic applications – A review," *Renew. Sustain. Energy Rev.*, vol. 94, pp. 1–14, 2018.
- [15] C. B. Jacobina, N. Rocha, G. A. de A. Carlos, and E. C. dos Santos, "Ac-Ac three-phase drive system based on twelve-leg de-link converter," in *2013 IEEE Energy Conversion Congress and Exposition*, 2013, pp. 2445–2452.
- [16] N. Mohamed, F. Aymen, Z. Issam, M. Bajaj, and S. S. M. Ghoneim, "The Impact of Coil Position and Number on Wireless System," *Sensors (Switzerland)*, vol. 21, no. 4343, pp. 1–19, 2021.
- [17] C. Spataro "Characterization of Measurements for Smart Grids" *International Journal Of Smart Grid - Ijsmartgrid*, Vol 7, no 4, 2023
- [18] T. Bouanou, H. El Fadil, A. Lassioui, O. Assaddiki, and S. Njili, "Analysis of coil parameters and comparison of circular, rectangular, and hexagonal coils used in wpt system for electric vehicle charging," *World Electr. Veh. J.*, vol. 12, no. 1, 2021.
- [19] M. Nishat Tasnim, S. Akter, M. Shahjalal, T. Shams, P. Davari, A. Iqbal, "A critical review of the effect of light duty electric vehicle charging on the power grid", *Energy Reports*, Vol. 10, 4126-4147, 2023,
- [20] H. Zhang, F. Lu, and C. Mi, "An electric roadway system leveraging dynamic capacitive wireless charging: Furthering the continuous charging of electric vehicles," *IEEE Electr. Mag.*, vol. 8, no. 2, pp. 52–60, 2020.
- [21] P. K. Joseph and D. Elangovan, "A review on renewable energy powered wireless power transmission techniques for light electric vehicle charging applications," *J. Energy Storage*, vol. 16, pp. 145–155, 2018.
- [22] M. Ibrahim, L. Pichon, L. Bernard, A. Razek, J. Houivet, and O. Cayol, "Advanced Modeling of a 2-kW Series-Series Resonating Inductive Charger for Real Electric Vehicle," *IEEE Transactions on Vehicular Technology*, vol. 64, no. 2, pp. 421–430, 2015.
- [23] C. S. Lee, J. B. Jeong, B. H. Lee, and J. Hur, "Study on 1.5 kW battery chargers for neighborhood electric vehicles," *2011 IEEE Veh. Power Propuls. Conf. VPPC 2011*, pp. 1–4, 2011.
- [24] A. Belkaid, I. Colak, K. Kayışli, and R. BAYINDIR, "Improving PV System Performance using High Efficiency Fuzzy Logic Control," in *2020 8th International Conference on Smart Grid (icSmartGrid)*, 2020, pp. 152–156.
- [25] G. A. Covic and J. T. Boys, "Inductive power transfer," *Proc.*

- IEEE*, vol. 101, no. 6, pp. 1276–1289, 2013.
- [26] J. Y. Lee and B. M. Han, "A bidirectional wireless power transfer EV charger using self-resonant PWM," *IEEE Trans. Power Electron.*, vol. 30, no. 4, pp. 1784–1787, 2015.
- [27] A. Abosaq, A. Belharith, A. Aldosari and A. Alzahrani, "Smart Solar Greenhouse Based Pldc", *11th IEEE International Conference On Smart Grid*, 2023
- [28] M. Yilmaz and P. T. Krein, "Review of battery charger topologies, charging power levels, and infrastructure for plug-in electric and hybrid vehicles," *IEEE Trans. Power Electron.*, vol. 28, no. 5, pp. 2151–2169, 2013.
- [29] Z. Bi, T. Kan, C. C. Mi, Y. Zhang, Z. Zhao, and G. A. Keoleian, "A review of wireless power transfer for electric vehicles: Prospects to enhance sustainable mobility," *Appl. Energy*, vol. 179, pp. 413–425, 2016.
- [30] C. Rami Reddy, K. Harinadha Reddy, F. Aymen, "Hybrid ROCOF Relay for Islanding Detection". *J. Electr. Eng. Technol.* 17, 51–60 (2022)
- [31] K. A. Kalwar, M. Aamir, and S. Mekhilef, "Inductively coupled power transfer (ICPT) for electric vehicle charging - A review," *Renew. Sustain. Energy Rev.*, vol. 47, pp. 462–475, 2015.
- [32] M. Naoui, F. Aymen, M. Ben Hamed, and S. Lassaad, "Analysis of Battery-EV state of charge for a Dynamic Wireless Charging system," *Energy Storage*, vol. 2, no. 2, pp. 1–10, 2019.
- [33] J. Zhao, T. Cai, S. Duan, H. Feng, C. Chen, and X. Zhang, "A General Design Method of Primary Compensation Network for Dynamic WPT System Maintaining Stable Transmission Power," *IEEE Trans. Power Electron.*, vol. 31, no. 12, pp. 8343–8358, 2016.
- [34] K. A. Kalwar, S. Mekhilef, M. Seyedmahmoudian, and B. Horan, "Coil design for high misalignment tolerant inductive power transfer system for EV charging," *Energies*, vol. 9, no. 11, pp. 12–17, 2016.
- [35] A. Babalhavaeji, H. Song, M. Radmanesh and M. Jalili, "Identifying electric vehicles from smart meter recordings," *2023 11th International Conference on Smart Grid (icSmartGrid), Paris, France, 2023*, pp. 1-3
- [36] F. Aymen and C. Mahmoudi, "A Novel Energy Optimization Approach for Electrical Vehicles in a Smart City," *Energies* 2019, Vol. 12, Page 929, vol. 12, no. 5, p. 929, Mar. 2019.
- [37] N. Mohamed, F. Aymen, Z. M. Ali, A. F. Zobaa, and S. H. E. A. Aleem, "Efficient Power Management Strategy of Electric Vehicles Based Hybrid Renewable Energy," *Sustain.*, vol. 13, no. 7351, pp. 1–20, 2021.
- [38] H. Turker, "Véhicules électriques Hybrides Rechargeables: évaluation des Impacts sur le Réseau électrique et Stratégies Optimales de recharge," Université de Grenoble, 2012.
- [39] S. Chopra, "Contactless Power Transfer for Electric Vehicle Charging Application," *Science (80)*, no. August, 2011.
- [40] N. Priyadarshi, M. S. Bhaskar, P. Sanjeevikumar, F. Azam, and B. Khan, "High-power DC-DC converter with proposed HSFNA MPPT for photovoltaic based ultra-fast charging system of electric vehicles," *IET Renew. Power Gener.*, 1-13, 2022.
- [41] N. Priyadarshi, S. Padmanaban, M. S. Bhaskar, and B. Khan, "An experimental performance verification of continuous mixed P-norm based adaptive asymmetrical fuzzy logic controller for single stage photovoltaic grid integration," *IET Renew. Power Gener.*, 1-11. 2022.
- [42] C. B. Nzoundja Fapi, H. Tchakounté, M. A. Hamida, P. Wira and M. Kamta, "Experimental Implementation of Improved P&O MPPT Algorithm based on Fuzzy Logic for Solar Photovoltaic Applications," *2023 11th International Conference on Smart Grid (icSmartGrid), Paris, France, 2023*, pp. 01-06.
- [43] T. T. Guingane, Z. Koalaga, E. Simonguy, F. Zougmore, and D. Bonkougou, "Modélisation et simulation d'un champ photovoltaïque utilisant un convertisseur élévateur de tension (boost) avec le logiciel MATLAB/SIMULINK," *J. Int. Technol. l'Innovation, la Phys. l'Energie l'Environnement*, vol. 2, no. 1, 2016.
- [44] M. Al-Tamimi and F. E. Alfaris, "Impact of Grid Impedance Characteristics on the Design Consideration of Utility-Scale PV Systems," *2023 11th International Conference on Smart Grid (icSmartGrid), Paris, France, 2023*, pp. 1-7
- [45] H. Kraiem, F. Aymen, L. Yahya, A. Triviño, M. Alharthi, and S. S. M. Ghoneim, "A Comparison between Particle Swarm and Grey Wolf Optimization Algorithms for Improving the Battery Autonomy in a Photovoltaic System," *Appl. Sci.*, vol. 11, no. 16, pp. 1–19, 2021.
- [46] S. Inoue, R. Nimri, A. Kamineni, and R. Zane, "A New Design Optimization Method for Dynamic Inductive Power Transfer Systems utilizing a Neural Network," in *2021 IEEE Energy Conversion Congress and Exposition (ECCE)*, 2021, pp. 1496–1501.